International Journal of Chemical, Materials and Biomolecular Sciences
ISSN: 2415-6620
Vol:10, No:8, 2016

Energy Deposited by Secondary Electrons Generated by Swift Proton Beams through Polymethylmethacrylate

Maurizio Dapor, Isabel Abril, Pablo de Vera, Rafael Garcia-Molina

***Abstract*—**The ionization yield of ion tracks in polymers and bio-molecular systems reaches a maximum, known as the Bragg peak, close to the end of the ion trajectories. Along the path of the ions through the materials, many electrons are generated, which produce a cascade of further ionizations and, consequently, a shower of secondary electrons. Among these, very low energy secondary electrons can produce damage in the biomolecules by dissociative electron attachment. This work deals with the calculation of the energy distribution of electrons produced by protons in a sample of polymethylmethacrylate (PMMA), a material that is used as a phantom for living tissues in hadron therapy. PMMA is also of relevance for microelectronics in CMOS technologies and as a photoresist mask in electron beam lithography. We present a Monte Carlo code that, starting from a realistic description of the energy distribution of the electrons ejected by protons moving through PMMA, simulates the entire cascade of generated secondary electrons. By following in detail the motion of all these electrons, we find the radial distribution of the energy that they deposit in PMMA for several initial proton energies characteristic of the Bragg peak.

***Keywords*—**Monte Carlo method, secondary electrons, energetic ions, ion-beam cancer therapy, ionization cross section, polymethylmethacrylate, proton beams, secondary electrons, radial energy distribution.

I. Introduction

INTERACTION of energetic ions with matter is present in many aspects of our daily lives. Cosmic radiation contains an enormous amount of projectiles [1], with 99% being atomic nuclei and about 1% being electrons. 90% of the atomic nuclei are hydrogen nuclei (protons), 9% alpha particles, and 1% nuclei of heavier elements. They produce showers of secondary particles that penetrate the atmosphere and can reach the surface of the Earth. Many of these particles can also reach delicate microelectronic devices present in spacecrafts, as well as their human crew [2]. Besides these potential hazards, energetic projectiles conveniently used can be employed to characterize and modify the properties of materials. Also, energetic ion beams represent a useful tool in radiotherapy [3]-[8]; in particular, ion-beam cancer therapy is based on the characteristic pattern of the energy deposited by ion beams in condensed targets. The depth-dose profile presents a sharp and narrow maximum, called Bragg peak, located at the end of the particle trajectory, close to the ions maximum range. This particular feature of the energy deposition pattern of ion beams is exploited to maximize the damage in the tumoral regions minimizing the effects of the irradiation on the healthy tissues near to the diseased cells [9].

From the point of view of modeling, the interaction of charged particles with condensed matter represents an intricate multi-scale problem. In particular, hadron therapy concerns biological materials, where the relevant bio-physical processes are very complex, as they involve reactions of nuclear fragmentation, secondary electron emission, damages to the cells, and repair mechanisms of macromolecules (e.g. DNA, proteins, etc.), among other processes [10].

It is known that a relevant part of the biological damage is due to the secondary electrons. In particular, the secondary electrons of very small energy play an important role in determining the damage, which they infringe by the dissociative electron attachment in the nascent stages of DNA radiolysis within cells [11], [12].

This work deals with the Monte Carlo calculation of the emission of secondary electrons [13] due to the energy delivered in the target by the swift proton beams. In particular, starting from a realistic description of the energy distribution of the electrons generated by protons moving through PMMA, which is used as a phantom of living tissues [14], we calculate the radial distribution of the energy deposited by the avalanche of secondary electrons, at energies typical around the Bragg peak. We assume that the secondary electron energy is deposited at depths where electrons interact with phonons or are trapped in the solid due to the polaronic effect. The determination of such radial energy deposition profiles is very relevant, for their influence in the response of the material to radiation, either for evaluating the biological effect in the case of radiotherapy, or the amount of damage, as well as its space resolution, in lithographic techniques.

The paper is structured as follows. In Section II, the theoretical methods used for this study are presented, including the formalism for calculating the energy spectrum of the ejected secondary electrons (Section II.A) and the Monte

M. D. is with the European Centre for Theoretical Studies in Nuclear Physics and Related Areas (ECT*), Bruno Kessler Foundation, and Trento Institute for Fundamental Physics and Applications (INFN-TIFPA), I-38123 Trento, Italy (corresponding author; phone: 39-0461-282037; fax: 39-0461-314501; e-mail: dapor@ ectstar.eu).

I. A. is with the Departament de Física Aplicada, Universitat d'Alacant, E-03080 Alacant, Spain (e-mail: ias@ua.es).

P. d. V. is with Department of Physical Sciences, The Open University, Walton Hall, MK7 6AA Milton Keynes, UK (e-mail: pablo.devera@open.ac.uk).

R. G.-M. is with Departamento de Física - Centro de Investigación en Óptica y Nanofísica, Regional Campus of International Excellence "Campus Mare Nostrum", Universidad de Murcia, E-30100 Murcia, Spain (e-mail: rgm@um.es).

Carlo code for following the cascade of electrons (Section II.B). The results are presented and discussed in Section III, while the final conclusions are given in Section IV.

II. Theoretical Framework

A. Electron Production by Primary Protons

The first step for the buildup of the radial energy deposition profile is the generation of secondary electrons by the primary energetic ion. An appropriate follow-up of the motion of the swift protons through the target can be accounted for in detail by means of the simulation code SEICS (Simulation of Energetic Ions and Clusters through Solids), which has been described elsewhere [15], [16], but whose main characteristics are summarized below.

By combining molecular dynamics and Monte Carlo techniques, the SEICS code incorporates the electronic energy-loss of the projectile (including stochastic fluctuations), multiple Coulomb scattering and elastic energy-loss, electron charge-exchange processes, as well as the nuclear fragmentation reactions induced by the incoming protons. The latter have been recently implemented [17] using the nuclear cross section data from the ICRU Report 63 [18] and a local energy deposition model. In this code, the electronic interactions are accounted for through realistic stopping cross sections calculated within the dielectric formalism and the MELF-GOS (Mermin Energy Loss Function - Generalized Oscillators Strengths) method [19]-[21], which provides a suitable description of the target electronic excitation spectrum from a physically motivated fitting to the available experimental optical data of the material, and its extension to arbitrary values of the momentum transfer.

The energy distribution of the electrons generated by each proton are obtained from the corresponding cross sections evaluated according to a semi-empirical model recently developed for biological targets and based on the dielectric formalism [22] that we summarize below. Let us consider a proton with kinetic energy T, moving through a condensed target characterized by its dielectric function $\varepsilon(k,\omega)$, where $\hbar k$ and $\hbar\omega$ are the momentum and energy transferred in an inelastic collision. The energy of the secondary electrons generated by the incoming proton is obtained assuming that the weakly-bound electrons of the target are characterized by a mean binding energy $\bar{B}$, such that, if an inelastic event occurs with $\hbar\omega > \bar{B}$, it implies that a secondary electron will be ejected with a kinetic energy $W = \hbar\omega - \bar{B}$. For the atom-like inner-shell electrons, characterized by their ionization energy $B_{\mathrm{ioniz},j}$, the secondary electrons will be emitted with a kinetic energy $W = \hbar\omega - B_{\mathrm{ioniz},j}$. The energy spectrum of the generated electrons by proton impact with energy T is obtained by the ionization single differential cross section (SDCS) $\frac{\mathrm{d}\sigma_{\mathrm{ioniz}}(T,W)}{\mathrm{d}W}$, given by [22]:

$$\frac{\mathrm{d}\sigma_{\mathrm{ioniz}}(T,W)}{\mathrm{d}W} = \frac{e^2M}{\pi\hbar^2TN}\int_{k_1}^{k_2}\frac{\mathrm{d}k}{k}\left\{\mathrm{Im}\left[\frac{-1}{\varepsilon(k,W+\bar{B})}\right]_{\mathrm{outer}}\sum_j \mathrm{Im}\left[\frac{-1}{\varepsilon(k,W+B_{\mathrm{ioniz},j})}\right]_{\mathrm{inner}}\right\} \quad (1)$$

where e is the fundamental charge, M is the proton mass, and N is the atomic density of the target. The integration limits are imposed by momentum conservation laws and they are given by $k_{2,1} = \sqrt{2M}\left(\sqrt{T} \pm \sqrt{T-\hbar\omega}\right)$. The first sum in the integrand refers to the outer shell electron excitations and the second one to the inner shell electron excitations. They both contribute to the energy loss function (ELF), $\mathrm{Im}\left(\frac{-1}{\varepsilon}\right)$, of the target.

Due to the interaction with the target atoms (electrons and nuclei), the proton energy degrades as it moves along the target. Therefore, the proton beam has an energy distribution that broadens as it reaches deeper regions in the target. As the ionization cross sections are function of the projectile energy, the energy spectra of the electrons generated along the proton track should be obtained by convoluting the energy distribution of the primary proton beam at each depth with the differential ionization cross section with respect to the electron ejection energy.

It is worth to notice that for the beams with the initial energies commonly used in hadron therapy (several hundred of MeV), primary protons around the Bragg peak have energies of a few MeV, and most of the initially generated electrons have low energies (several tens of eV) [17].

B. Secondary Electron Propagation Simulation

The propagation of the generated electrons by proton impact was simulated by using an appropriate Monte Carlo code, that takes both elastic and inelastic interactions into account. The treatment of the elastic collisions is based on the differential and total elastic scattering cross sections calculated utilizing Mott theory [23], i.e. numerically solving the Dirac equation in a central field; this procedure is known as the "relativistic partial wave expansion method" and it has been demonstrated to provide excellent results when compared to experimental data [24]-[29].

Concerning the energy losses, the inelastic mean free path was calculated by taking into account the inelastic interactions of the incident electrons with atomic electrons, with phonons, and with polarons.

The calculation of the electron-electron inelastic scattering processes was performed within the dielectric formalism and the Mermin theory [30]. Electron-phonon interactions were described using the Fröhlich theory [31], [32]. The polaronic effect was modeled according to the law proposed by Ganachaud and Mokrani [33], which parameters where determined by the best comparison of the Monte Carlo code results to a set of experimental data.

Electron trajectories follow a stochastic process, with scattering events separated by straight paths having a distribution of lengths that follows a Poisson-type law. Once the step length is generated, the elastic or inelastic nature of the next scattering event, the polar and azimuthal angles, and the energy losses, are all sampled by using the relevant cumulative probabilities according to the usual Monte Carlo recipes [34], [35]. Details of the present Monte Carlo calculations can be found in [36].

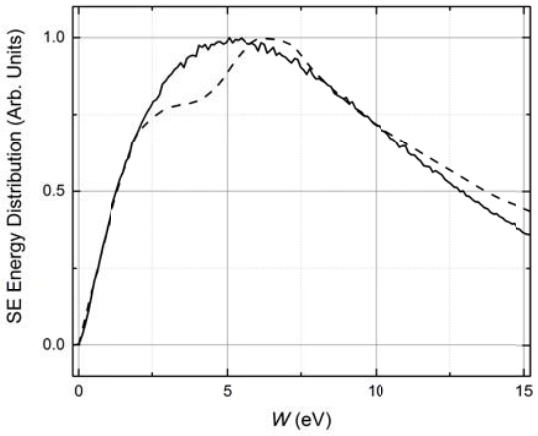

Fig. 1 Energy distribution of the secondary electrons ejected from PMMA after being generated an electron beam incident with 1 keV normal to the surface. Monte Carlo simulated data (solid line) are compared to the Joy et al. experimental spectrum [37] (dashed line)

In Fig. 1, we compare to the Joy et al. experimental data [37] the Monte Carlo simulated spectrum of the secondary electrons (SEs) escaping from PMMA with energies in the range from 0 to 15 eV, after being generated by a 1 keV electron incident normally to the target surface. The same conditions of the experiment are used for the simulation, i.e. normal incidence, primary energy equal to 1 keV, and acceptance angles in the range from 36° to 48° integrated around the full 360° azimuth (Cylindrical Mirror Analyzer geometry). The zero of the energy scale is located at the vacuum level. The Monte Carlo calculation describes well the initial increase of the spectrum, the position of the maximum (Monte Carlo position of the maximum is ~5.4 eV while the experimental one is ~6 eV) and the full width at half maximum FWHM (around 11-12 eV both in the experiment and in the simulation). However, further work is required to improve the Monte Carlo algorithm for an interpretation of the experimental details observed close to the maximum in the low energy part of the spectrum [38], [39].

III. Results and Discussion

A. Generation of Secondary Electrons by Proton Impact

In Fig. 2, we show the energy distribution of the secondary electrons generated by the proton impact with energies of 1 and 5 MeV. We choose these representative energies because they match with those of protons around the Bragg peak when the initial beam energies correspond to those employed in hadron therapy. These calculations are obtained from (1) where the MELF-GOS model is used to describe the ELF of PMMA over the complete energy and momentum transfer range [40], as explained in the previous section.

We find that most of the secondary electrons generated by the proton impact are in the low-energy range of several tens of eV (see Fig. 2), what is quantified by the average energy of the ejected electrons given by:

$$W_{\mathrm{aver}}(T) = \frac{1}{\sigma_{\mathrm{ioniz}}(T)} \int_0^{W_{\max}} W \frac{\mathrm{d}\sigma_{\mathrm{ioniz}}(T,W)}{\mathrm{d}W} \mathrm{d}W \quad (2)$$

where $\sigma_{\mathrm{ioniz}}(T)$ is the total ionization cross section and $W_{\max} = 4mT/M$ is the maximum energy transferred in a collision, and m is the electron mass.

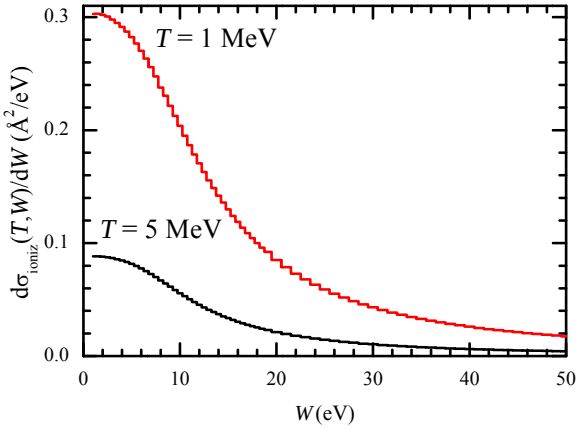

Fig. 2 Energy distribution of secondary electrons (ionization SDCS) produced by energetic protons of T = 1 and 5 MeV in PMMA, as a function of the kinetic energy of the emitted electrons

We find that the average electron energy increases with the proton energy, obtaining that it is 42 eV for 1 MeV protons and 50 eV for 5 MeV. On the other hand, the initial total energy deposited by the generated electrons by proton impact is around 3.11 times bigger for 1 MeV protons compared with 5 MeV protons.

The ionization SDCS increases when the proton energy decreases, obtaining that the maximum value of $\frac{\mathrm{d}\sigma_{\mathrm{ioniz}}(T,W)}{\mathrm{d}W}$ is 3.42 times larger for 1 MeV protons than for 5 MeV protons. It is also interesting to compare the number of electrons generated by the protons at different energies, which is proportional to the total ionization cross section. We find that the number of secondary electrons generated for 1 MeV protons is around 3.72 times larger than for 5 MeV protons.

B. Propagation of the Secondary Electrons

The simulation of the transport of the secondary electron emission follows the entire cascade of electrons, which lose energy via the three following processes: (*i*) Secondary electron emission; in this process, no energy is deposited to the material: the energy lost by the originating electron is transferred to the secondary electron and transported away. (*ii*) Phonon creation; this process is responsible of energy deposition to the material. (*iii*) Polaron creation and trapping of the electron; this process is responsible of energy deposition to the material as well [41].

The energy transferred to each secondary electron is transported away from the site where the collision occurred, with the energy being deposited into the material only where each secondary electron interacted with phonons or was trapped in the solid due to the polaronic effect.

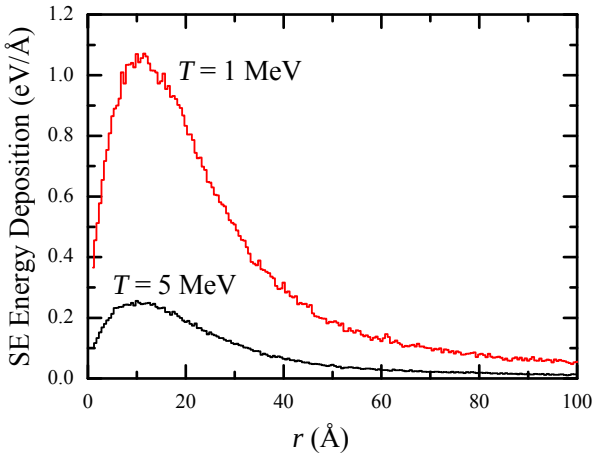

Fig. 3 Monte Carlo simulation of the radial energy deposited by secondary electrons produced by a 1 MeV and 5 MeV proton beam impinging on PMMA, as a function of the radial distance *r* from the ion impact. The energy is deposited in spherical shells of inner radius *r* and outer radius *r* +d *r*

In Fig. 3, we present the Monte Carlo calculation of the secondary electron radial energy distribution for PMMA irradiated by a 1.0 MeV and 5.0 MeV proton beams.

The calculated distribution was obtained assuming that the primary electrons emerge from the proton track according to the ionization cross section corresponding to the electron energy distributions reported in the previous subsection. Their cumulative probabilities were used to calculate the initial energy of each primary electron. The radial distribution for 1 MeV protons was normalized to one initial electron. The radial distribution corresponding for 5 MeV protons were scaled according to the number of secondary electrons ejected at each energy. The scaling factor for 1 MeV protons is 3.72 times larger than it is for 5 MeV protons.

The results shown in Fig. 3 allow establishing the shape of the energy distribution of the secondary electrons in PMMA and the mean distance from the proton track reached by the energy deposited. Such a distance defines the target area likely to be damaged by the secondary electrons. The radial distribution of deposited energy has a maximum around 10-12 Å from the ion track and then decays exponentially.

IV. Conclusion

Starting from a realistic description of the energy distribution of the electrons ejected by protons moving through PMMA obtained by the dielectric formalism and the MELF-GOS method, a quantitative Monte Carlo technique was used to calculate the electron-energy deposition (due to the entire cascade of the generated electrons) around the ion track. The energy was assumed to be deposited where electrons interact with phonons or are trapped in the solid due to polaronic effect. Proceeding in this manner, we found the radial distribution of the energy that all the secondary electrons deposit in the polymer PMMA along the proton track. This is one of the main features affecting the response of the material under irradiation.

Acknowledgment

MD wishes to express warm thanks to Giovanni Garberoglio (ECT*-LISC, Trento) for his stimulating suggestions. Monte Carlo simulations of secondary electron emission were performed on the KORE cluster at FBK. We also thank financial support provided by the Spanish Ministerio de Economía y Competitividad and the European Regional Development Fund (Project No. FIS2014-58849-P) and the Fundación Séneca (Project No. 19907/GERM/15). PdV acknowledges financial support from the European Union's FP7-People Program (Marie Curie Actions) within the Initial Training Network No. 608163 "ARGENT".

References

[1] L. Anchordoqui, T. Paul, S. Reucroft, and J. Swain, "The Neutron Flux Variation in the Earth's Atmosphere Depending on the Solar Proton Flux", *Int. J. Modern Physics A* 18, 2229-2366 (2003).
[2] F. A. Cucinotta, M.-. Y. Kim, L. J. Chappell, J. L. Huff, "How Safe Is Safe Enough? Radiation Risk for a Human Mission to Mars", *PLos ONE* 8, e74988 (2013).
[3] T. Kanai, Y. Furusawa, K. Fukutsu, H. Itsukaichi, K. Eguchi-Kasai, and H. Ohara, "Irradiation of Mixed Beam and Design of Spread-Out Bragg Peak for Heavy-Ion Radiotherapy", *Radiation Research* 147, 78-85 (1997).
[4] M. Krämer, O. Jäkel, T. Haberer, G. Kraft, D. Schardt, and U. Weber, "Treatment planning for heavy-ion radiotherapy: physical beam model and dose optimization", *Phys. Med. Biol.* 45, 3299-3317 (2000).
[5] I. Turesson, K.-A. Johansson, and S. Mattsson, "The Potential of Proton and Light Ion Beams in Radiotherapy", *Acta Oncologica* 42, 107-114 (2003).
[6] A. Brahme, "Recent Advances in Light Ion Radiation Therapy", International Journal of Radiation Oncology • Biology • Physics 58, 603-616 (2004).
[7] D. Schulz-Ertner and H. Tsujii, "Particle Radiation Therapy using Proton and Heavier Ion Beams", *J. Clinical Oncology* 25, 953-964 (2007).
[8] T. Elsässer, W. K. Weyrather, T. Friedrich, M. Durante, G. Iancu, M. Krämer, G. Kragl, S. Brons, M. Winter, K.-J. Weber, M. Scholz, "Quantification of the Relative Biological Effectiveness for Ion Beam Radiotherapy: Direct Experimental Comparison of Proton and Carbon Ion Beams and a Novel Approach for Treatment Planning", *Int. J. Radiation Oncology, Biology, Physics* 78, 1177-1183 (2010).
[9] R. Baskar, K. A. Lee, R. Yeo, and K-W. Yeoh, "Cancer and Radiation Therapy: Current Advances and Future Directions", *Int. J. Med. Sci.* 9, 193-199 (2012).
[10] E. Surdutovich and A. V. Solov'yov, "Multiscale approach to the physics of radiation damage with ions", *Eur. Phys. J. D* 68, 353 (30 pp) (2014).
[11] B. Boudaïffa, P. Cloutier, D. Hunting, M. A. Huels, and L. Sanche, "Resonant formation of DNA strand breaks by low-energy (3 to 20 eV) electrons", *Science* 287, 1658-1660 (2000).
[12] X. Pan, P. Cloutier, D. Hunting, and L. Sanche, "Dissociative Electron Attachment to DNA", *Phys. Rev. Lett.* 90, 20812 (4 pp) (2003).
[13] M. Dapor, M. Ciappa, and W. Fichtner, "Monte Carlo Modeling in the Low-Energy Domain of the Secondary Electron Emission of Polymethylmethacrylate for Critical Dimension Scanning Electron Microscopy", *J. Micro/Nano MEMS, MOEMS* 9, 023001 (9 pp) (2010).
[14] International Commission on Radiation Units and Measurements. Measurement of Dose Equivalents from external photon and electron Radiations. ICRU Report 47. Bethesda, Maryland (1992).
[15] R. Garcia-Molina, I. Abril, S. Heredia-Avalos, I. Kyriakou, and D. Emfietzoglou, "A combined molecular dynamics and Monte Carlo simulation of the spatial distribution of energy deposition by proton beams in liquid water", *Phys. Med. Biol.* 56, 6475-6493 (2011).
[16] R. Garcia-Molina, I. Abril, P. de Vera, I. Kyriakou, and D. Emfietzoglou, "Proton beam irradiation of liquid water: A combined molecular dynamics and Monte Carlo simulation study of the Bragg peak profile", ch. 8 (pp. 271-304) in *Fast Ion-Atom and Ion-Molecule*

Collisions, ed. by, Dž. Belkic (World Scientific Publishing Company, Singapore, 2012).
[17] P. de Vera, I. Abril, and R. Garcia-Molina, to be published (2016).
[18] International Commission on Radiation Units and Measurements. Nuclear Data for Neutron and Proton Radiotherapy and for Radiation Protection, ICRU Report 63. Bethesda, Maryland (2000).
[19] I. Abril, R. Garcia-Molina, C. D. Denton, F. J. Pérez-Pérez, and N. R. Arista, "Dielectric description of wakes and stopping powers in solids", *Phys. Rev. A* 58, 357-366 (1998).
[20] S. Heredia-Avalos, R. Garcia-Molina, J. M. Fernández-Varea, and I. Abril, "Calculated energy loss of swift He, Li, B, and N ions in SiO_2, Al_2O_3, and ZrO_2", *Phys. Rev. A* 72, 052902 (9 pp) (2005).
[21] R. Garcia-Molina, I. Abril, I. Kyriakou, D. Emfietzoglou, in *Radiation Damage in Biomolecular Systems, Biological and Medical Physics, Biomedical Engineering*, edited by G. G. Gómez-Tejedor, M. C. Fuss (Springer, Dordrecht, 2012), ch. 15.
[22] P. de Vera, R. Garcia-Molina, I. Abril I, and A. V. Solov'yov, "Semiempirical Model for the Ion Impact Ionization of Complex Biological Media", *Phys. Rev. Lett.* 110, 148104 (5 pp) (2013).
[23] N. F. Mott, "The Scattering of Fast Electrons by Atomic Nuclei", *Proc. R. Soc. London Ser.* 124, 425-442 (1929).
[24] S.-R. Lin, N. Sherman, and J. K. Percus, "Elastic scattering of relativistic electrons by screened atomic nuclei", *Nucl. Phys.* 45, 492-504 (1963).
[25] P. J. Bunyan and J. L. Shonfelder, "Polarization by Mercury of 100 to 2000 eV Electrons", *Proc. Phys. Soc.* 85, 455-462 (1965).
[26] F. Salvat and R. Mayol, "Elastic scattering of electrons and positrons by atoms. Schrödinger and Dirac partial wave analysis" *Comput. Phys. Commun.* 74 , 358-374 (1993).
[27] M. Dapor, "Elastic Scattering Calculations for Electrons and Positrons in Solid Targets", *J. Appl. Phys.* 79, 8406-8411 (1996).
[28] M. Dapor, *Electron-Beam Interactions with Solids: Applications of the Monte Carlo Method to Electron Scattering Problems*, Vol. 186 of Springer Tracts in Modern Physics, Springer, Berlin, 2003.
[29] A. Jablonski, F. Salvat and C. J. Powell, "Comparison of Electron Elastic-Scattering Cross Sections Calculated from Two Commonly Used Atomic Potentials", *J. Phys. Chem. Ref. Data* 33, 409-451 (2004).
[30] N. D. Mermin, "Lindhard Dielectric Function in the Relaxation-Time Approximation", Phys. Rev. B 1, 2362-2363 (1970).
[31] H. Fröhlich, "Electrons in Lattice Fields", *Adv. Phys.* 3, 325-361 (1954).
[32] J. Llacer and E. L. Garwin, "Electron-Phonon Interaction in Alkali Halides. I. The Transport of Secondary Electrons with Energies between 0.25 and 7.5 eV", *J. Appl. Phys.* 40, 2766-2775 (1969).
[33] J. P. Ganachaud and A. Mokrani, "Theoretical Study of the Secondary Electron Emission of Insulating Targets", *Surf. Sci.* 334, 329-341 (1995).
[34] R. Shimizu and Ze-Jun Ding, "Monte Carlo Modelling of Electron-Solid Interactions", *Rep. Prog. Phys.* 55, 487-531 (1992).
[35] J. Ch. Kuhr and H. J. Fitting, "Monte Carlo Simulation of Electron Emission from Solids", J. Electron Spectrosc. Relat. Phenom. 105, 257-273 (1999).
[36] M. Dapor, *Transport of Energetic Electrons in Solids: Computer Simulation with Applications to Materials Analysis and Characterization*, Vol. 257 of Springer Tracts in Modern Physics, Springer, Berlin, 2014.
[37] D. C. Joy, M. S. Prasad, H. M. Meyer III, "Experimental Secondary Electron Spectra under SEM Conditions", *Journal of Microscopy* 215, 77-85 (2004).
[38] M. Dapor, *Appl. Surf. Sci.* to be published (2016).
[39] M. Dapor, *G.I.T. Imaging & Microscopy*, to be published (2016).
[40] P. de Vera, I. Abril, R. Garcia-Molina, "Inelastic Scattering of Electron and Light Ion Beams in Organic Polymers", *J. Appl. Phys.* 109, 094901 (8 pp) (2011).
[41] M. Dapor, I. Abril, P. de Vera, and R. Garcia-Molina, "Simulation of the secondary electrons energy deposition produced by proton beams in PMMA: Influence of the target electronic excitation description", *Eur. Phys. J. D* 69, 165 (10 pp) (2015).